MedChemComm

Accepted Manuscript

This is an *Accepted Manuscript*, which has been through the Royal Society of Chemistry peer review process and has been accepted for publication.

Accepted Manuscripts are published online shortly after acceptance, before technical editing, formatting and proof reading. Using this free service, authors can make their results available to the community, in citable form, before we publish the edited article. We will replace this *Accepted Manuscript* with the edited and formatted *Advance Article* as soon as it is available.

You can find more information about *Accepted Manuscripts* in the Information for Authors.

Please note that technical editing may introduce minor changes to the text and/or graphics, which may alter content. The journal's standard Terms & Conditions and the Ethical guidelines still apply. In no event shall the Royal Society of Chemistry be held responsible for any errors or omissions in this *Accepted Manuscript* or any consequences arising from the use of any information it contains.

ROYAL SOCIETY OF CHEMISTRY

www.rsc.org/medchemcomm

Cite this: DOI: 10.1039/c0xx00000x

www.rsc.org/xxxxxx

ARTICLE TYPE

Synthesis and biological evaluation of a new class of quinazolinone azoles as potential antimicrobial agents and their interactions with calf thymus DNA and human serum albumin

Li-Ping Peng, Sangaraiah Nagarajan†, Syed Rasheed‡, Cheng-He Zhou*

Received (in XXX, XXX) Xth XXXXXXXXX 20XX, Accepted Xth XXXXXXXXX 20XX
DOI: 10.1039/b000000x

A series of novel quinazolinone azoles were synthesized and characterized by NMR, IR, MS and HRMS spectra. Bioactive assay showed that some target compounds exhibited significant antimicrobial potency. Especially, nitroimidazole derivative **3a** displayed comparable or even better antibacterial efficacies (MIC = 0.03–0.05 μmol/mL) in contrast with norfloxacin (MIC = 0.01–0.05 μmol/mL) and chloromycin (MIC = 0.02–0.10 μmol/mL). The preliminary interactive investigations of compound **3a** with calf thymus DNA by UV-vis spectroscopic method revealed that compound **3a** could bind to DNA to form compound **3a**-DNA complex by an intercalative mode and further block DNA replication to exert their powerful antibacterial and antifungal activities. The hydrogen bonds and van der Waals forces played important roles in the association of compound **3a**-HSA.

1. Introduction

Quinolones are a well known class of synthetic antimicrobial drugs with excellent safety profile, favorable pharmacokinetic characteristics and broad antibacterial spectrum. It is generally considered that quinolones can bind with the enzyme-DNA binary complex to form ternary complexes, thereby blocking DNA replication and leading to bacterial cells' death. Since the first generation of quinolone drugs was found to be active in the early 1960s, four generations of quinolones have been clinically used in succession, such as nalidixic acid, pipemidic acid, lomefloxacin, moxifloxacin and so on. [1] Nevertheless, the prevalently clinical use of this class of anti-infective drugs has led to increasingly worrisome resistance at a disturbing rate. [2] Furthermore, their shortcomings including phototoxicity, lipid peroxidation, photohemolysis and bad water-solubility also limit the administrable mode. [3] This situation stimulates the urgent need to design and develop powerful antimicrobial quinolone agents, [4] especially for the exploration of new quinolone-like compounds. Quinazolinones with benzopyrimidone skeleton are a type of important compounds structurally similar to clinical benzopyridone quinolone drugs. Reasonably, a great deal of work has recently been directed towards quinazolinone compounds and the related research has become increasingly active. [5]

Quinazolinones have been found to possess extensively biological activities [5] such as antibacterial, [6] antifungal, [7] antiviral, [8] antiinflammatory, [9] antimalarial, [10] antioxidant, [11] antimycobacterial, [12] anticancer properties [13] and so on. Numerous efforts have been devoted to the research and development of quinazolinones as potential medicinal drugs by the separation and purification of naturally occurring alkaloids from a variety of plants as well as artificial synthesis of quinazolinone compounds with novel structures and properties. So far some quinazolinones, for example, methaqualone as a hypnotic and anticonvulsant agent and quinethazone as a diuretic drug have been used in clinic. [5a] More importantly, an increasing number of quinazolinone compounds have displayed great potency in the treatment of microbial infections. [5,14]

Azole compounds such as mono-nitrogen thiazoles, [15] oxazoles [16] and carbazoles, [17] bis-nitrogen imidazoles [18] and benzimidazoles, [19] tri-nitrogen triazoles [20] and benzotriazoles, [21] and tetra-nitrogen tetrazoles [22] are an important class of nitrogen heterocycles with multiple heteroatoms, aromaticity and electron rich property. Their special structure endows azole-based derivatives easily bind with the enzymes and receptors in organisms through noncovalent interactions such as coordination and hydrogen bonds, thereby possessing various applications in medicinal chemistry, [23] especially their protrudent effects such as imidazoles [4a,18,24] and triazoles [4b,20,25] against microbial strains. In recent years, some work has manifested that the introduction of some nitrogen-containing heterocyclic moieties such as pyrazole and thiazole into quinazolinone backbone can significantly increase the antimicrobial efficiency and broaden their antimicrobial spectrum. [5,26] However, to the best of our knowledge, other quinazolinone azoles have been seldom

Institute of Bioorganic & Medicinal Chemistry, School of Chemistry and Chemical Engineering, Southwest University, Chongqing 400715, China
** Corresponding authors; E-mail: zhouch@swu.edu.cn (C. H. Zhou); Tel.: +86-23-68254967; Fax: +86-23-68254967*
† Postdoctoral fellow from School of Chemistry, Madurai Kamaraj University, India
‡ Postdoctoral fellow from Department of Chemistry, Hyderabad University, India

Medicinal Chemistry Communications Accepted Manuscript

reported. In view of the above observations and as an extension of our studies on the development of azole compounds, herein we incorporated different azole fragments into the *N*-3 position of quinazolinone to generate a novel class of quinazolinone azoles. Research provides evidence that alkyl linkers can modulate the physicochemical properties and thus improve biological potency. [27] With the aim of better understanding of structure-activity relationship and increasing flexibilities, different lengths of alkyl chains were introduced into the target compounds to investigate the influences of linkers on bioactive profiles. The prepared compounds might be expected to exhibit potential activities against bacterial and fungal strains including drug-resistant microorganisms. Therefore, their antibacterial and antifungal potency for all newly synthesized compounds were evaluated *in vitro* against four Gram-positive bacteria including Methicillin-Resistant *Staphylococcus aureus* N315 (MRSA), four Gram-negative bacteria and five fungi. The preliminary antimicrobial mechanism was investigated by evaluating the interactions of the prepared highly active compound with calf thymus DNA. [28] It is well accepted that the overall distribution, metabolism, and efficacies of drugs can be changed by their affinity to human serum albumin (HSA), and many promising new drugs have been rendered ineffective because of their unusually high affinity to this protein. [29] So the full investigations of interactions between drugs or bioactive small molecules and HSA not only provide a proper understanding of the absorption, transportation, distribution, metabolism and excretion properties of drugs, but also are helpful to design, modify and screen drug molecules. [30] Thus, further binding behaviors between the synthesized active compound and HSA were investigated to evaluate their transportation and pharmacokinetic properties by fluorescence and UV-vis absorption spectroscopy.

2. Chemistry

The target quinazolinone azoles were synthesized according to the synthetic route outlined in Scheme 1. Commercially available fluoro or chloro substituted 2-aminobenzoic acid was reacted with formamidine acetate in the presence of 2-methoxyethanol to produce 7-fluoroquinazolin-4(3*H*)-one or 7-chloroquinazolin-4(3*H*)-one **1a-b** in high yield of 80%, and then compounds **1a-b** were further treated with a series of alkyl dibromides in acetone using potassium carbonate as base to afford bromides **2a-j** with the yields of 50–76% according to the previously reported method. [31] The target quinazolinone azoles **3a-j**, **4a-j** and **5a-d** were conveniently and efficiently obtained in 50–67% yields by the reaction of bromides **2a-j** respectively with 2-methyl-5-nitroimidazole, 4-nitroimidazole, imidazole or triazole in acetonitrile at 50 ºC in the presence of potassium carbonate as base. Unfortunately, under the same condition above, imidazoles **5a-b** were obtained in relatively low yields, which demonstrated that potassium carbonate was unfavorable for this reaction, probably its basicity was too weak to form imidazole carbanion. Therefore, sodium hydride was selected as base in the reaction of imidazole with bromides, which easily afforded the imidazole derivatives **5a-b** with good yields ranging from 58% to 69% at 50 ºC in anhydrous tetrahydrofuran under a stream of nitrogen. All the new compounds were confirmed by ^{1}H NMR, ^{13}C NMR, IR, MS and HRMS spectra (Supporting Information 1).

3. Results and discussion

3.1. Antimicrobial activities

The obtained results (Supporting Information 2) as depicted in Table 1 revealed that quinazolinone nitroimidazoles **3a-j** could effectively inhibit the growth of all the tested bacterial strains except for *P. aeruginosa*, while triazole compounds **5c-d** showed potent activity against *M. luteus* and *P. aeruginosa*.

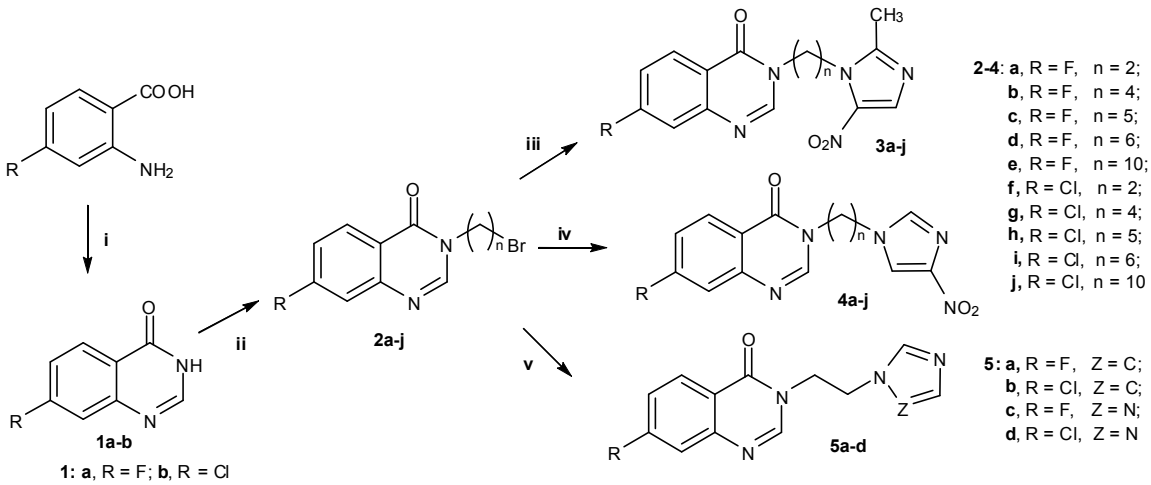

Scheme 1 Synthetic routes of quinazolinone azoles. Reagents and conditions: (i) formamidine acetate, 2-methoxyethanol, reflux, 18 h; (ii) alkyl dibromides, K_2CO_3, acetone, 50 ºC, 5 h; (iii) 2-methyl-5-nitroimidazole, K_2CO_3, acetonitrile, 50 ºC, 5 h; (iv) 4-nitroimidazole, K_2CO_3, acetonitrile, 50 ºC, 5 h; (v) imidazole or triazole, K_2CO_3, acetonitrile, 50 ºC, 5 h.

Especially the hybrid of quinazolinone and 2-methyl-5-nitroimidazole **3a** gave comparable or even superior antibacterial efficacies (MIC = 0.03–0.05 μmol/mL) to norfloxacin (MIC = 0.01–0.05 μmol/mL) and chloromycin (MIC = 0.02–0.10 μmol/mL). 4-Nitroimidazoles **4a-j** showed stronger anti-*B. subtilis* activity (MIC = 0.02–0.05 μmol/mL) than chloromycin (MIC = 0.10 μmol/mL). The results also showed that intermediates **2a-j** and imidazoles **5a-b** displayed weak or no obvious activities in inhibiting the growth of microorganisms. The fluoro or chloro substituent of quinazolinone at C-7 position

This journal is © The Royal Society of Chemistry [year]

Medicinal Chemistry Communications Accepted Manuscript

did not exert significantly different influence on antimicrobial potency.

It was known that MRSA was one of the most virulent organisms that showed severe multi-drug resistance to numerous currently available agents. Excitingly, 2-methyl-5-nitroimidazoles **3a-j** could effectively inhibit the growth of MRSA at the concentrations of 0.02–0.05 μmol/mL, which were comparable or even more active in comparison with clinical chloromycin (MIC = 0.05 μmol/mL). The results in Table 2 also demonstrated the great effects of alkyl chain lengths on biological activities. Long-chain alkyl 4-nitroimidazoles **4c-e** and **4h-j** possessed better antimicrobial activities than short-chain derivatives **4a-b** and **4f-g** against most of the tested strains, respectively. Particularly for *B. subtilis*, compounds **4c-e** with $(CH_2)_5$, $(CH_2)_6$ and $(CH_2)_{10}$ linkers respectively were five-fold more potent (MIC = 0.02 μmol/mL) than chloromycin (MIC = 0.10 μmol/mL). This might be explained by the high hydrophobicity of long alkyl chain, making it easy to penetrate the cytomembrane and therefore improve the antibacterial activity.

The antifungal evaluation *in vitro* revealed that most of nitroimidazole compounds showed antifungal efficiency to some extent, which were similar to the antibacterial results. Noticeably, 2-methyl-5-nitroimidazoles **3a-j** showed good inhibitory efficiency against all the tested fungal strains, which further implied the fact that nitroimidazole nucleus was in favor of antimicrobial potency. Especially, compound **3d** with $(CH_2)_6$ linker could efficiently inhibit the growth of *A. flavus* strain *in vitro* with MIC value of 0.01 μmol/mL, which was 84-fold more potent than fluconazole (MIC = 0.84 μmol/mL). The results suggested that this compound may be further investigated as anti-*A. flavus* agent.

Table 1. *In vitro* antimicrobial data as MIC (μmol/mL)[a, b, c] for compounds **2–5**

Compds	Fungi					Gram-positive bacteria				Gram-negative bacteria			
	C. utilis	*A. flavus*	*B. yeast*	*C. albicans*	*C. mycoderma*	*M. luteus*	MRSA	*S. aureus*	*B. subtilis*	*P. aeruginosa*	*E. coli*	*B. proteus*	*E. typhosa*
2a	0.94	1.89	0.94	0.94	>1.89	0.47	0.94	>1.89	1.89	>1.89	1.89	0.47	>1.89
2b	0.43	1.71	0.86	0.86	>1.71	0.86	0.43	>1.71	1.71	>1.71	1.71	0.86	>1.71
2c	0.41	0.82	0.82	0.82	>1.63	0.41	0.82	>1.63	1.63	>1.63	1.63	0.41	>1.63
2d	0.39	1.56	0.78	0.78	>1.56	0.39	0.39	>1.56	1.56	>1.56	0.78	0.39	>1.56
2e	0.33	1.34	0.67	0.67	>1.34	0.67	0.33	>1.34	1.34	>1.34	1.34	0.33	>1.34
2f	0.89	>1.78	0.89	>1.78	>1.78	0.45	0.89	>1.78	1.78	>1.78	1.78	0.89	>1.78
2g	0.41	>1.62	0.81	>1.62	>1.62	0.81	0.81	>1.62	1.62	>1.62	0.81	0.41	>1.62
2h	0.39	>1.55	0.78	>1.55	>1.55	0.39	0.78	>1.55	1.55	>1.55	1.55	0.39	>1.55
2i	0.74	>1.49	0.74	>1.49	>1.49	0.37	0.74	>1.49	1.49	>1.49	1.49	0.74	>1.49
2j	0.32	>1.28	0.64	>1.28	>1.28	0.32	0.64	>1.28	1.28	>1.28	0.64	0.32	>1.28
3a	0.03	0.03	0.03	0.03	0.03	0.05	0.03	0.03	0.03	>1.61	0.03	0.05	0.03
3b	0.05	0.02	0.05	0.02	0.05	0.05	0.02	0.05	0.05	>1.48	0.05	0.02	0.02
3c	0.02	0.02	0.02	0.04	0.04	0.02	0.02	0.04	0.02	>1.42	0.04	0.02	0.02
3d	0.02	0.01	0.04	0.02	0.02	0.04	0.04	0.04	0.02	>1.37	0.04	0.04	0.02
3e	0.02	0.04	0.02	0.04	0.02	0.04	0.02	0.02	0.02	>1.19	0.02	0.02	0.02
3f	0.05	0.02	0.05	0.05	0.05	0.10	0.05	0.10	0.05	>1.53	0.10	0.05	0.02
3g	0.02	0.04	0.04	0.02	0.04	0.04	0.02	0.04	0.04	>1.42	0.04	0.02	0.02
3h	0.02	0.02	0.04	0.02	0.02	0.04	0.02	0.04	0.02	>1.36	0.02	0.02	0.02
3i	0.02	0.04	0.02	0.02	0.02	0.04	0.02	0.02	0.04	>1.31	0.04	0.02	0.02
3j	0.02	0.02	0.04	0.02	0.04	0.02	0.04	0.02	0.02	>1.15	0.02	0.02	0.02
4a	0.42	>1.69	0.21	0.05	0.84	0.05	0.21	0.84	0.05	>1.69	0.84	0.42	0.42
4b	0.39	0.77	0.10	0.10	0.77	0.05	0.19	0.39	0.05	0.77	0.77	0.39	0.39
4c	0.37	0.74	0.09	0.09	0.19	0.05	0.19	0.19	0.02	0.37	0.37	0.37	0.37
4d	0.36	0.18	0.09	0.04	0.04	0.04	0.18	0.36	0.02	0.36	0.18	0.09	0.36
4e	0.15	0.15	0.08	0.04	0.04	0.04	0.15	0.31	0.02	0.08	0.15	0.08	0.31
4f	0.40	>1.60	0.20	0.10	0.80	0.05	0.20	0.80	0.05	>1.60	0.80	0.40	0.40
4g	0.37	0.74	0.09	0.09	0.74	0.05	0.18	0.37	0.05	0.74	0.74	0.37	0.37
4h	0.35	0.71	0.09	0.09	0.18	0.04	0.18	0.18	0.04	0.35	0.35	0.35	0.35
4i	0.34	0.17	0.09	0.04	0.04	0.04	0.17	0.34	0.04	0.34	0.17	0.09	0.34
4j	0.15	0.15	0.07	0.04	0.04	0.04	0.15	0.30	0.04	0.07	0.15	0.07	0.30
5a	0.99	0.50	0.50	0.99	>1.98	0.50	0.99	>1.98	>1.98	0.99	1.98	1.98	>1.98
5b	0.47	0.93	0.93	0.93	>1.86	0.47	0.93	>1.86	>1.86	0.93	1.86	1.86	>1.86
5c	0.99	0.99	0.49	0.99	0.49	0.03	0.49	0.99	0.49	0.03	0.25	0.99	0.99
5d	0.46	0.93	0.46	0.93	0.46	0.03	0.46	0.93	0.46	0.03	0.23	0.93	0.93
A	>1.58	>1.58	>1.58	>1.58	>1.58	0.02	0.05	0.05	0.10	0.10	0.10	0.10	0.10
B	>1.60	>1.60	>1.60	>1.60	>1.60	0.01	0.03	0.01	0.01	0.01	0.05	0.01	0.01
C	0.03	0.84	0.05	<0.01	0.01	>1.67	>1.67	>1.67	>1.67	>1.67	>1.67	>1.67	>1.67

[a] Minimum inhibitory concentrations were determined by micro broth dilution method for microdilution plates.

[b] *C. utilis, Candida utilis* ATCC9950*; A. flavus, Aspergillus flavus* ATCC204304*; B. yeast, Beer yeast* ATCC9763*; C. albicans, Candida albicans* ATCC10231*; C. mycoderma, Candida mycoderma* ATCC9888*; M. luteus, Micrococcus luteus* ATCC4698*;* MRSA*, Methicillin-Resistant Staphylococcus aureus* N315*; S. aureus, Staphylococcus aureus* ATCC25923*; B. subtilis*, *Bacillus subtilis* ATCC6633; *P. aeruginosa, Pseudomonas aeruginosa* ATCC27853*; E. Coli, Escherichia coli* DH52*; B. proteus*, *Bacillus proteus* ATCC13315; *E. typhosa, Eberthella typhosa* ATCC14028.

[c] A = chloromycin; B = norfloxacin; C = fluconazole.

3.2 Interactions with calf thymus DNA

Deoxyribonucleic acid (DNA) is the informational molecule encoding the genetic instructions used in the development and

Medicinal Chemistry Communications Accepted Manuscript

function of almost all known living organisms. It is one of the targets for the studies of biologically important small molecules such as antimicrobial drugs. The binding studies of small molecules with DNA are important and helpful for developing novel and more efficient drugs, which have been attracting considerable attention in biomedical science. To explore the possible antimicrobial action mechanism, the binding behavior of active compound **3a** with calf thymus DNA (a DNA model with medical importance, low cost and ready availability properties) was studied on molecular level *in vitro* using neutral red (NR) dye as a spectral probe by UV-vis spectroscopic methods. [32]

3.2.1 Absorption spectra of DNA in the presence of compound 3a

The use of absorption spectroscopy is quite useful technique in DNA-binding studies. In absorption spectroscopy, hypochromism and hyperchromism are very important spectral features to distinguish the change of DNA double-helical structure. [33] Due to the strong interactions between the electronic states of intercalating chromophore and that of the DNA base, the observed large hyperchromism strongly suggests a close proximity of the aromatic chromophore to the DNA bases. With a fixed concentration of DNA, UV-vis absorption spectra were recorded with the increasing amount of compound **3a**. As shown in Figure 1, UV-vis spectra displayed that the maximum absorption peak of DNA at 260 nm exhibited proportional increase with the increasing concentration of compound **3a**. Meanwhile the absorption value of **3a**-DNA complex was a little greater than the measured value of simply sum of free DNA and free compound **3a**. These meant a weak hyperchromism effect existed between DNA and compound **3a**. Furthermore, the intercalation of the aromatic chromophore of compound **3a** into the helix and the strong overlap of π-π* states in the large π-conjugated system with the electronic states of DNA bases were consistent with the observed spectral changes.

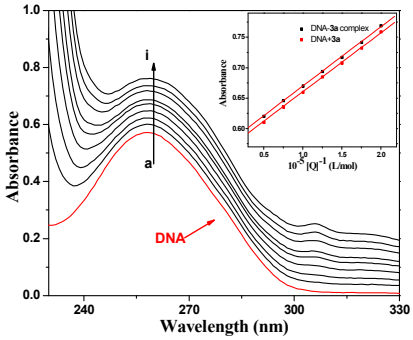

Figure 1 UV absorption spectra of DNA with different concentrations of compound **3a** (pH = 7.4, T = 290 K). Inset: comparison of absorption at 260 nm between the **3a**-DNA complex and the sum values of free DNA and free compound **3a**. c(DNA) = 8.62 × 10^{-5} mol/L, and c(compound **3a**) = 0–2.0 × 10^{-5} mol/L for curves *a*-*i* respectively at increment 0.25 × 10^{-5}.

On the basis of the variations in the absorption spectra of DNA upon binding to **3a**, equation 1 can be utilized to calculate the intrinsic binding constant (K).

$$\frac{A^0}{A-A^0}=\frac{\xi_C}{\xi_{D-C}-\xi_C}+\frac{\xi_C}{\xi_{D-C}-\xi_C}\times\frac{1}{K[Q]} \qquad (1)$$

A^0 and A represent the absorbance of DNA in the absence and presence of compound **3a** at 260 nm, ξ_C and $\xi_{D\text{-}C}$ are the absorption coefficients of compound **3a** and **3a**-DNA complex respectively. The plot of $A^0/(A\text{-}A^0)$ versus 1/[compound **3a**] is constructed by using the absorption titration data and linear fitting (Figure 2), yielding the binding constant, K = 1.41 × 10^4 L/mol, R = 0.998, SD = 0.34 (R is the correlation coefficient, and SD is standard deviation).

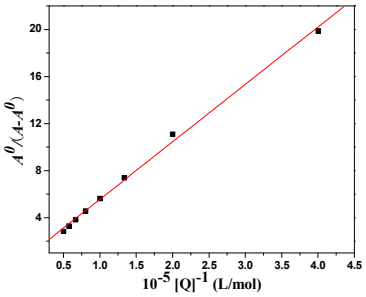

Figure 2 The plot of $A^0/(A\text{-}A^0)$ versus 1/[compound **3a**]

3.2.2 Absorption spectra of NR interactions with DNA

Neutral Red (NR) is a planar phenazine dye and structurally similar to other planar dyes such as acridines, thiazines and xanthenes, which shows lower toxicity, higher stability and convenient application. Furthermore, it has been sufficiently demonstrated by spectrophotometric and electrochemical techniques that the binding of NR with DNA is an intercalation binding. [28b] Therefore, NR was employed as a spectral probe to investigate the binding mode of **3a** with DNA in the present work. The absorption spectra of the NR dye upon the addition of DNA were shown in Figure 3. It was apparent that the absorption peak of the NR at around 460 nm displayed gradual decrease with the increasing concentration of DNA, and a new band at around 530 nm developed. This was attributed to the formation of the new DNA-NR complex. An isosbestic point at about 504 nm provided evidence of DNA-NR complex formation.

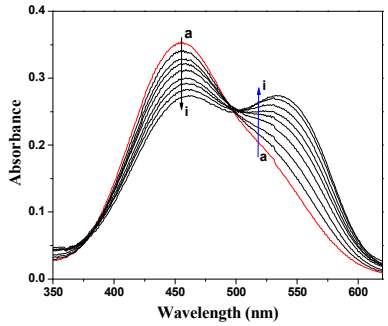

Figure 3 UV absorption spectra of NR in the presence of DNA at pH 7.4 and room temperature. c(NR) = 2.0 × 10^{-5} mol/L, and c(DNA) = 0–5.25 × 10^{-5} mol/L for curves *a*-*i* respectively at increment 0.66 × 10^{-5}.

3.2.3 Absorption spectra of competitive interactions of compound 3a and NR with DNA

Figure 4 displayed the absorption spectra of a competitive binding between NR and **3a** with DNA. As shown, with the increasing concentration of **3a**, the maximum absorption around 460 nm of the DNA-NR complex increased. Compared with the absorption band at around 460 nm of the free NR in the presence of the increasing concentrations of DNA (Figure 3), the spectra in Figure 4 (inset) exhibited the reverse process. The results

Medicinal Chemistry Communications Accepted Manuscript

This journal is © The Royal Society of Chemistry [year]

suggested that compound **3a** intercalated into the double helix of DNA by substituting for NR in the DNA-NR complex.

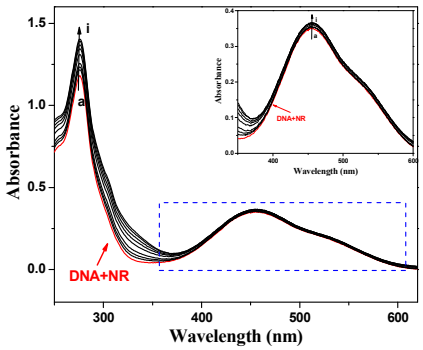

Figure 4 UV Absorption spectra of the competitive reaction between **3a** and neutral red with DNA. c(DNA) = 4.31 × 10^{-5} mol/L, c(NR) = 2.0 × 10^{-5} mol/L, and c(compound **3a**) = 0–2.0 × 10^{-5} mol/L for curves *a-i* respectively at increment 0.25 × 10^{-5}. (Inset) Absorption spectra of the system with the increasing concentration of **3a** in the wavelength range of 350–600 nm absorption spectra of competitive reaction between compound **3a** and NR with DNA.

3.3 Interactions of compound 3a with HSA

HSA is the most abundant serum proteins in the systemic circulation comprising about 60% in plasma and provides about 80% of the colloid osmotic pressure of blood. Full investigations of interactions of drugs with HSA are not only beneficial to thoroughly understand the pharmacokinetic behavior of drugs, but also to design, modify and screen drug molecules. [30]

3.3.1 UV-vis absorption spectral study

UV-vis absorption measurement is a very easy operational method applicable to explore the structural change of protein and to identify the complex formation. In our binding experiment, UV-vis absorption spectroscopic method was adopted to evaluate the binding behaviors between compound **3a** and HSA. As shown in Figure 5, the absorption peak observed at 278 nm was attributed to the aromatic rings in Tryptophan (Trp-214), Tyrosine (Tyr-411) and Phenylalanine (Phe) residues in HSA. With the addition of compound **3a**, the peak intensity increased, indicating that compound **3a** could interact with HSA and the peptide strands of HSA were extended. However, the maximum absorption wavelength remained unchanged, implying that the interactions of compound **3a** and HSA were a noncovalent interaction. It occurred *via* the π-π stacking between aromatic rings of compound **3a** and Trp, Tyr and Phe residues, which possessed conjugated π-electrons and located in the binding cavity of HSA. [34]

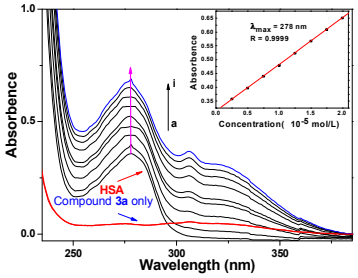

Figure 5 Effect of compound **3a** to HSA UV-vis absorption, c(HSA) = 1.0 × 10^{-5} mol/L; c(compound **3a**)/(10^{-5} mol/L): 0, 0.25, 0.5, 0.75, 1, 1.25, 1.5, 1.75, 2 (T = 298 K, pH = 7.40). The inset corresponds to the absorbance at 278 nm with different concentrations of compound **3a**.

3.3.2 Fluorescence quenching mechanism

Fluorescence spectroscopy is also an effective method to study the interactions of small molecules with HSA. The fluorescence intensity of Trp-214 may change when HSA interacts with other small molecules, which could be reflected in the fluorescence spectra of HSA in the UV region. The effect of compound **3a** on the fluorescence intensity to HSA at 298 K was shown in Figure 6 (Supporting Information 3). It was obvious that HSA had a strong fluorescence emission with a peak at 358 nm owing to the single Try-214 residue. The intensity of this characteristic broad emission band regularly decreased with the increased concentrations of compound **3a**, but the maximum emission wavelength of HSA remained unchanged. This suggested that Trp-214 did not undergo any change in polarity. [29b]

The fluorescence quenching data can be analyzed by the well-known Stern-Volmer equation: [35]

$$\frac{F_0}{F} = 1 + K_{SV}[Q] = 1 + K_q\tau_0[Q] \qquad (2)$$

Where F_o and F represent fluorescence intensity in the absence and presence of compound **3a**, respectively. K_{SV} (L/mol) is the Stern-Volmer quenching constant, K_q is the bimolecular quenching rate constant (L mol^{-1} s^{-1}), τ_0 is the fluorescence lifetime of the fluorophore in the absence of quencher, assumed to be 6.4×10^{-9} s for HSA, and [Q] is the concentration of compound **3a**. Hence, the Stern-Volmer plots of HSA in the presence of compound **3a** at different concentrations and temperatures could be calculated and were shown in Figure 7.

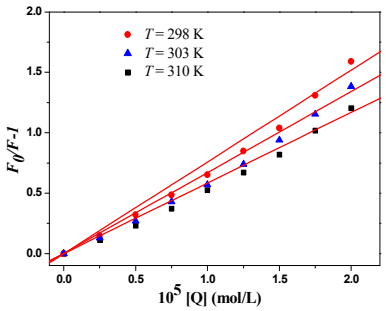

Figure 7 Stern-Volmer plots of **3a**-HSA system at different temperatures

Fluorescence quenching occurs by different mechanisms, usually classified as dynamic quenching and static quenching depending on temperature and viscosity. Because higher temperatures result in larger diffusion coefficients, the quenching constants are expected to increase with a gradually increasing temperature in dynamic quenching. However, the increase of temperature is likely to result in a smaller static quenching constant due to the dissociation of weakly bound complexes.

The values of K_{SV} and K_q for the interactions of compound **3a** with HSA at different temperatures were shown in Table 2 (Supporting Information 3). The K_{SV} values were inversely correlated with the temperature, which indicated that the fluorescence quenching of HSA was probably initiated by the formation of **3a**-HSA complex rather than dynamic collisions. The K_q values obtained at different temperatures were in the range of 10^{12}–10^{13} L/mol s^{-1}, which far exceeded the diffusion controlled rate constants of various quenchers with a biopolymer

Medicinal Chemistry Communications Accepted Manuscript

(2.0×10^{10} L/mol s^{-1}), and indicated that the quenching was not initiated by the dynamic diffusion process but occurred in the statical formation of **3a**-HSA complex.

3.3.3 Binding constant and site

For a static quenching process, the data could be described by the Modified Stern-Volmer equation: [36]

$$\frac{F_0}{\Delta F} = \frac{1}{f_a K_a}\frac{1}{[Q]} + \frac{1}{f_a} \qquad (3)$$

Where ΔF is the difference in fluorescence intensity in the absence and presence of compound **3a** at concentration $[Q]$, f_a is the fraction of accessible fluorescence, and K_a is the effective quenching constant for the accessible fluorophores, which are analogous to associative binding constants for the quencher-acceptor system. The dependence of $F_o/\Delta F$ on the reciprocal value of quencher concentration $[Q]^{-1}$ is linear with the slope equaling to the value of $(f_a K_a)^{-1}$. The value f_a^{-1} is fixed on the ordinate. The constant K_a is a quotient of the ordinate f_a^{-1} and the slope $(f_a K_a)^{-1}$. The Modified Stern-Volmer plots were shown in Figure 8 and the calculated results were depicted in Table 3 (Supporting Information 3).

When small molecules bind to a set of equivalent sites on a macromolecule, the equilibrium binding constants and the numbers of binding sites can also be calculated according to the Scatchard equation: [37]

$$r/D_f = nK_b - rK_b \qquad (4)$$

Where D_f is the molar concentration of free small molecules, r is the moles of small molecules bound per mole of protein, n is binding sites multiplicity per class of binding sites, and K_b is the equilibrium binding constant. The Scatchard plots were shown in Figure 9 and the K_b and n were listed in Table 3 (Supporting Information 3).

Figure 9 showed the Modified Stern-Volmer and Scatchard plots for the **3a**-HSA system at different temperatures. The decreased trend of K_a and K_b with increased temperatures was in accordance with K_{SV}'s depended on temperatures. The value of the binding site n was approximately 1, which showed one high affinity binding site was present in the interactions of compound **3a** with HSA. The results also showed that the binding constants were moderate and the effects of temperatures were not significant, thus compound **3a** might be stored and carried by this protein.

3.3.4 Binding mode and thermodynamic parameters

Generally, there are four types of non-covalent interactions including hydrogen bonds, van der Waals forces, electrostatic interactions and hydrophobic bonds, which play important roles in small molecules binding to proteins. [38] The thermodynamic parameters enthalpy (ΔH) and entropy (ΔS) change of binding reaction are the main evidence for confirming the interactions between small molecules and protein. If the ΔH does not vary significantly over the studied temperatures range, then its value and ΔS can be evaluated from the van't Hoff equation:

$$\ln K = -\frac{\Delta H}{RT} + \frac{\Delta S}{R} \qquad (5)$$

Where K is analogous to the associative binding constants at the corresponding temperature and R is the gas constant. In order to explain the binding model between compound **3a** and HSA, the thermodynamic parameters were calculated from the van't Hoff plots. The ΔH was estimated from the slope of the van't Hoff relationship (Figure 10, Supporting Information 3). The free energy change (ΔG) was then calculated from the following equation:

$$\Delta G = \Delta H - T\Delta S \qquad (6)$$

Table 4 (Supporting Information 3) summarized the values of ΔH, ΔG and ΔS. The negative values of free energy ΔG of the interactions between compound **3a** and HSA suggested that the binding process was spontaneous. The negative entropy ΔS and enthalpy ΔH values of the interactions of compound **3a** with HSA indicated that the binding was mainly enthalpy-driven and the entropy was unfavorable for it, moreover, hydrogen bonds and van der Waals forces played a major role in the reaction.

4. Conclusion

In conclusion, a novel class of quinazolinone azoles were successfully synthesized in good yields *via* an easy, convenient and efficient synthetic route. All the newly synthesized compounds were characterized by ^{1}H NMR, ^{13}C NMR, MS, IR and HRMS spectra. The biological results revealed that some target compounds exhibited significant antibacterial and antifungal activities against most of the tested strains. Especially nitroimidazole derivative **3a** gave comparable or even better antibacterial efficacies (MIC = 0.03–0.05 μmol/mL) in contrast with norfloxacin (MIC = 0.01–0.05 μmol/mL) and chloromycin (MIC = 0.02–0.10 μmol/mL). The specific interactions of compound **3a** with DNA were studied by UV-vis absorption spectroscopy. Experimental results displayed that compound **3a** could intercalate DNA to form compound **3a**-DNA complex which might further block DNA replication to exert their powerful antibacterial and antifungal activities. The calculated parameters indicated that the binding process was spontaneous, and hydrogen bonds and van der Waals forces played important roles in the strong association of compound **3a**-HSA. Further research, including the *in vivo* bioactive evaluation along with toxicity investigation and the effect factors on antimicrobial activities such as other heterocyclic rings [23a,39] (benzotriazole, benzimidazole and their derivatives etc.) as well as spacers with different types of linkers (aralkyl, aryl and heterocyclic types and their lengths of chains) are active in progress. All these will be discussed in a future paper.

Acknowledgments

This work was partially supported by National Natural Science Foundation of China (No. 21172181, 21372186), the Research Fellowship for International Young Scientists from International (Regional) Cooperation and Exchange Program (No. 81350110523, 81450110095), the key program from Natural Science Foundation of Chongqing (CSTC2012jjB10026) and the Specialized Research Fund for the Doctoral Program of Higher Education of China (SRFDP 20110182110007) and Chongqing Special Fund for Postdoctoral Research Proposal (Xm2014127).

Medicinal Chemistry Communications Accepted Manuscript

This journal is © The Royal Society of Chemistry [year]

Notes and References

1 (a) C. Mugnaini, S. Pasquini and F. Corelli, *Curr. Med. Chem.*, 2009, **16**, 1746–1767; (b) A. Ahmed and M. Daneshtalab, *J. Pharm. Pharmaceut. Sci.*, 2012, **15**, 52–72.

2 K. J. Aldred, R. J. Kerns and N. Osheroff, *Biochemistry*, 2014, **53**, 1565–1574.

3 J. A. Wiles, B. J. Bradbury and M. J. Pucci, *Expert Opin. Ther. Patents*, 2010, **20**, 1295–1319.

4 (a) S. F. Cui, L. P. Peng, H. Z. Zhang, S. Rasheed, K. V. Kumar and C. H. Zhou, *Eur. J. Med. Chem*., 2014, **86**, 318–334: (b) F. W. Zhou, H. S. Lei, L. Fan, L. Jiang, J. Liu, X. M. Peng, X. R. Xu, L. Chen, C. H. Zhou, Y. Y. Zou, C. P. Liu, Z. Q. He and D. C. Yang, *Bioorg. Med. Chem. Lett.*, 2014, **24**, 1912–1917; (c) S. F. Cui, Y. Ren, S. L. Zhang, X. M. Peng, G. L. V. Damu, R. X. Geng and C. H. Zhou, *Bioorg. Med. Chem. Lett.*, 2013, **23**, 3267–3272; (d) Y. Wang, G. L. V. Damu, J. S. Lv, R. X. Geng, D. C. Yang and C. H. Zhou, *Bioorg. Med. Chem. Lett.*, 2012, **22**, 5363–5366.

5 (a) P. C. Sharma, G. Kaur, R. Pahwa, A. Sharma and H. Rajak, *Curr. Med. Chem*., 2011, **18**, 4786–4812; (b) I. Khan, A. Ibrar, N. Abbas and A. Saeed, *Eur. J. Med. Chem*., 2014, **76**, 193–244; (c) R. Rajput and A. P. Mishra, *Int. J. Pharm. Pharm. Sci*., 2012, **4**, 66–70.

6 X. Wang, J. Yin, L. Shi, G. P. Zhang and B. A. Song, *Eur. J. Med. Chem*., 2014, **77**, 65–74.

7 X. Wang, Z. N. Li, J. Yin, M. He, W. Xue, Z. W. Chen and B. A. Song, *J. Agr. Food Chem*., 2013, **61**, 9575–9582.

8 (a) Z. W. Wang, M. X. Wang, X. Yao, Y. Li, J. Tan, L. Z. Wang, W. T. Qiao, Y. Q. Geng, Y. X. Liu and Q. M. Wang, *Eur. J. Med. Chem*., 2012, **53**, 275–282; (b) A. L. Leivers, M. Tallant, J. B. Shotwell, S. Dickerson, M. R. Leivers, O. B. McDonald, J. Gobel, K. L. Creech, S. L. Strum, A. Mathis, S. Rogers, C. B. Moore and J. Botyanszki, *J. Med. Chem*., 2014, **57**, 2091–2106.

9 M. F. Zayed and M. H. Hassan, *Saudi Pharm. J*., 2014, **22**, 157–162.

10 Y. Takeuchi, M. Koike, K. Azuma, H. Nishioka, H. Abe, S. H. Kim, Y. Wataya and T. Harayama, *Chem. Pharm. Bull*., 2001, **49**, 721–725.

11 A. A. Al-Amiery, A. A. H. Kadhum, M. Shamel, M. Satar, Y. Khalid and A. B. Mohamad, *Med. Chem. Res*., 2014, **23**, 236–242.

12 M. B. Patel, U. Harikrishnan, N. N. Valand, N. R. Modi and S. K. Menon, *Arch. Pharm. Chem. Life Sci*., 2013, **346**, 210–220.

13 C. Carmi, E. Galvani, F. Vacondio, S. Rivara, A. Lodola, S. Russo, S. Aiello, F. Bordi, G. Costantino, A. Cavazzoni, R. R. Alfieri, A. Ardizzoni, P. G. Petronini and M. Mor, *J. Med. Chem*., 2012, **55**, 2251–2264.

14 (a) F. A. M. Al-Omary, G. S. Hassan, S. M. El-Messery, M. N. Nagid, E. E. Habib and H. I. El-Subbagh, *Eur. J. Med. Chem*., 2013, **63**, 33–45; (b) L. P. Shi, K. M. Jiang, J. J. Jiang, Y. Jin, Y. H. Tao, K. Li, X. H. Wang and J. Lin, *Bioorg. Med. Chem. Lett.*, 2013, **23**, 5958–5963; (c) N. C. Desai, H. V. Vaghani and P. N. Shihora, *J. Fluorine Chem*., 2013, **153**, 39–47.

15 (a) S. F. Cui, Y. Wang, J. S. Lv, G. L. V. Damu and C. H. Zhou, *Scientia Sinica Chimica*, 2012, **42**, 1105–1131 (in Chinese); (b) S. F. Cui, C. H. Zhou, R. X. Geng and Q. G. Ji, *Chin. J. Biochem. Pharm*. 2012, **33**, 311–315 (in Chinese).

16 H. Z. Zhang, C. H. Zhou, R. X. Geng and Q. G. Ji, *Chin. J. Org. Chem.*, 2011, **31**, 1963–1976 (in Chinese).

17 (a) F. F. Zhang, C. H. Zhou and J. P. Yan, *Chin. J. Org. Chem.*, 2010, **30**, 783–796 (in Chinese); (b) F. F. Zhang, L. L. Gan and C. H. Zhou, *Bioorg. Med. Chem. Lett*., 2010, **20**, 1881–1884.

18 (a) L. Zhang, X. M. Peng, G. L. V. Damu, R. X. Geng and C. H. Zhou, *Med. Res. Rev*., 2014, **34**, 340–437; (b) L. Zhang, J. J. Chang, S. L. Zhang, G. L. V. Damu, R. X. Geng and C. H. Zhou, *Bioorg. Med. Chem.*, 2013, **21**, 4158–4169.

19 (a) H. Z. Zhang, S. F. Cui, S. Nagarajan, S. Rasheed, G. X. Cai and C. H. Zhou, *Tetrahedron Lett.*, 2014, **55**, 4105–4109; (b) H. Z. Zhang, J. M. Lin, S. Rasheed and C. H, Zhou, *Sci. China Chem.*, 2014, **57**, 807–822; (c) S. L. Zhang, G. L. V. Damu, L. Zhang, R. X. Geng and C. H. Zhou, *Eur. J. Med. Chem.*, 2012, **55**, 164–175.

20 (a) C. H. Zhou and Y. Wang, *Curr. Med. Chem.*, 2012, **19**, 239–280; (b) H. Z. Zhang, G. L. V. Damu, G. X. Cai and C. H. Zhou, *Curr. Org. Chem.*, 2014, **18**, 359–406; (c) Y. Y. Zhang, J. L. Mi, C. H. Zhou and X. D. Zhou. *Eur. J. Med. Chem.,* 2011, **46**, 4391–4402; (d) Q. P. Wang, J. Q. Zhang, G. L. V. Damu, K. Wan, H. Z. Zhang and C. H. Zhou, *Sci. China Chem.*, 2012, **55**, 2134–2153.

21 (a) Y. Shi, C. H. Zhou, X. D. Zhou, R. X. Geng and Q. G. Ji, *Acta Pharm. Sin*. 2011, **46**, 798–810 (in Chinese); (b) Y. Shi and C. H. Zhou, *Bioorg. Med. Chem. Lett*., 2011, **21**, 956–960.

22 (a) L. L. Dai, S. F. Cui, G. L. V. Damu and C. H. Zhou, *Chin. J. Org. Chem.*, 2013, **33**, 224–244 (in Chinese); (b) L. L. Dai, H. Z. Zhang, S. Nagarajan, S. Rasheed and C. H. Zhou. *Med. Chem. Comm*., 2014, DOI: 10.1039/C4MD00266K.

23 (a) X. M. Peng, G. X. Cai and C. H. Zhou, *Curr. Top. Med. Chem.*, 2013, **13**, 1963–2010; (b) S. L. Zhang, J. J. Chang, G. L. V. Damu, R. X. Geng and C. H. Zhou. *Med. Chem. Comm*., 2013, **4**, 839–846; (c) Y. Y. Zhang and C. H. Zhou, *Bioorg. Med. Chem. Lett*., 2011, **21**, 4349–4352; (d) S. Li, J. X. Chen, Q. X. Xiang, L. Q. Zhang, C. H. Zhou, J. Q. Xie, L.Yu and F. Z. Li, *Eur. J. Med. Chem*., 2014**, 84**, 677–686; (e) C. H. Zhou, Y. Y. Zhang, C. Y. Yan, K. Wan, L. L. Gan and Y. Shi, *Anti-Cancer Agents Med. Chem.,* 2010, **10**, 371–395; (f) C. H. Zhou, L. L. Gan, Y. Y. Zhang, F. F. Zhang, G. Z. Wang, L. Jin and R. X. Geng, *Sci. China, Ser B: Chem*., 2009, **52**, 415–458.

24 (a) G. L. V. Damu, S. F. Cui, X. M. Peng, Q. M. Wen, G. X. Cai and C. H. Zhou, *Bioorg. Med. Chem. Lett.*, 2014**, 24**, 3605–3608; (b) B. Fang, C. H. Zhou and X. C. Rao, *Eur. J. Med. Chem*., 2010, **45**, 4388–4398; (c) G. L. V. Damu, Q. P. Wang, H. Z. Zhang, Y. Y. Zhang, J. S. Lv and C. H. Zhou, *Sci. China Chem.*, 2013, **56**, 952–969.

25 (a) Y. Wang and C. H. Zhou, *Scientia Sinica Chimica*, 2011, **41**, 1429–1456 (in Chinese); (b) J. J. Wei, Y. Wang, X. L.Wang, C. H. Zhou and Q. G. Ji, *Chin. Pharm. J.*, 2011, **46**, 481–485 (in Chinese); (c) S. L. Zhang, J. J. Chang, G. L. V. Damu, B. Fang, X. D. Zhou, R. X. Geng and C. H. Zhou, *Bioorg. Med. Chem. Lett*., 2013, **23**, 1008–1012; (d) J. S. Lv, X. M. Peng, B. Kishore and C. H. Zhou, *Bioorg. Med. Chem. Lett*., 2014, **24**, 308–313; (e) H. Z. Zhang, J. J. Wei, K. V. Kumar, S. Rasheed and C. H. Zhou, *Med. Chem. Res*., 2014, DOI: 10.1007/s00044–014–1123–9.

26 K. A. M. El-Bayouki, M. M. Aly, Y. A. Mohamed, W. M. Basyouni and Y. S. Abbas, *World J. Chem*., 2009, **4**, 161–170.

27 (a) X. L. Wang, K. Wan and C. H. Zhou, *Eur. J. Med. Chem.*, 2010, **45**, 4631–4639; (b) Y. Luo, Y. H. Lu, L. L. Gan, C. H. Zhou, J. Wu, R. X. Geng and Y. Y. Zhang, *Arch. Pharm. Chem. Life. Sci*., 2009, **342**, 386–393.

28 (a) G. W. Zhang, P. Fu, L. Wang and M. M. Hu, *J. Agric. Food Chem.*, 2011, **59**, 8944–8952; (b) X. L. Li, Y. J. Hu, H. Wang, B. Q. Yu and H. L. Yue, *Biomacromolecules*, 2012, **13**, 873–880.

29 (a) F. Berti, S. Bincoletto, I. Donati, G. Fontanive, M. Fregonese and F. Benedetti, *Org. Biomol. Chem.*, 2011, **9**, 1987–1999; (b) Y. J. Hu, Y. Liu and X. H. Xiao, *Biomacromolecules*, 2009, **10**, 517–521.

30 D. C. Carter and J. X. Ho, *Adv. Protein Chem.*, 1994, **45**, 153–203.

31 (a) J. W. Cusic and E. F. Levon, *N*-[2-(nitro-1-imidazolyl)ethyl]naphthal imides, US Pat. 3997572, 1976; (b) K. Lee, J. Kim, K. Jeong, K. W. Lee, Y. Lee, J. Y. Song, M. S. Kim, G. S. Lee and Y. Kim, *Bioorg. Med. Chem.*, 2007, **17**, 3152–3161.

32 A. J. Berdis, *Biochemistry*, 2008, **47**, 8253–8260.

33 C. D. Kanakis, S. Nafisi, M. Rajabi, A. Shadaloi, P. A. Tarantilis, M. G. Polissiou, J. Bariyanga and H. A. Tajmir-Riahi, *Spectroscopy*, 2009, **23**, 29–43.

34 V. D. Suryawanshi, P. V. Anbhule, A. H. Gore, S. R. Patil and G. B. Kolekar, *Ind. Eng. Chem. Res.*, 2012, **51**, 95–102.

35 J. R. Lakowicz, Principles of fluorescence spectroscopy, third ed., Springer, New York, 2006, pp. 11–12.

36 B. T. Yin, C. Y. Yan, X. M. Peng, S. L. Zhang, S. Rasheed, R. X. Geng and C. H. Zhou, *Eur. J. Med. Chem.*, 2014, **71**, 148–159.

37 J. Y. Yang and W. Y. Yang, *J. Am. Chem. Soc.*, 2009, **131**, 11644–11645.

38 U. S. Mote, S. R. Patil, S. H. Bhosale, S. H. Han and G. B. Kolekar, *Photochem. Photobiol. B*, 2011, **103**, 16–21.

39 (a) X. M. Peng, G. L. V. Damu and C. H. Zhou, *Curr. Pharm. Des.*, 2013, **19**, 3884–3930; (b) H. Z. Zhang, G. L. V. Damu, G. X. Cai and C. H. Zhou, *Eur. J. Med. Chem.*, 2013, **64**, 329–344.

Medicinal Chemistry Communications Accepted Manuscript